

# Beyond the temporal Tsirelson bound: an experimental test of a Leggett-Garg inequality in a three-level system

Kunkun Wang,<sup>1</sup> Clive Emary,<sup>2</sup> Xiang Zhan,<sup>1</sup> Zhihao Bian,<sup>1</sup> Jian Li,<sup>1</sup> and Peng Xue<sup>1,3,\*</sup>

<sup>1</sup>*Department of Physics, Southeast University, Nanjing 211189, China*

<sup>2</sup>*Joint Quantum Centre (JQC) Durham-Newcastle,  
School of Mathematics and Statistics, Newcastle University,  
Newcastle-upon-Tyne, NE1 7RU, United Kingdom*

<sup>3</sup>*State Key Laboratory of Precision Spectroscopy,  
East China Normal University, Shanghai 200062, China*

The Leggett-Garg inequalities hold under the assumptions of macrorealism but can be violated by quantum mechanics. The degree to which quantum systems can violate these inequalities, however, is bounded. In particular, if the measurements on the system are genuinely dichotomic, the bound for these temporal inequalities is the same as Tsirelson bound for the relevant spatial Bell inequality. In this paper we realise a photonic Leggett-Garg test on a three-level system and implement ideal negative measurements that admit three distinct measurement outcomes. In this way we obtain violations of a Leggett-Garg inequality significantly in excess of the temporal Tsirelson bound. This underlines the difference between Bell and Leggett-Garg inequalities and hence spatial and temporal correlations in quantum mechanics. We also report violations of a quantum-witness equality up to the maximum permitted for a three-level system.

In contrast to Bell inequalities which probe correlations between multiple spatially-separated systems [1, 2], the Leggett-Garg inequalities (LGIs) test the temporal correlations of a single system [3, 4]. The LGIs are based on two assumptions that intuitively hold in the world of our everyday experience: (i) *macroscopic realism* — that a system exists at all times in a macroscopically-distinct state; and (ii) *non-invasive measurability* — that it is possible to measure a system without disturbing it. Since both these assumptions fails under quantum mechanics, quantum systems can violate the LGIs. Hence the use of these inequalities as indicators of quantum coherence, in particular in macroscopic systems [5].

The simplest LGI concerns the correlation functions of a dichotomic variable  $Q(t) = \pm 1$  at pairs of three times  $t_i$ ;  $i = 1, 2, 3$ , and can be written [4]

$$K \equiv \langle Q(t_2)Q(t_1) \rangle + \langle Q(t_3)Q(t_2) \rangle - \langle Q(t_3)Q(t_1) \rangle \leq 1.$$

This inequality, or its close relatives, have been tested and violated in many experiments, with most studies having been performed on two-level quantum systems, e.g. [6–18]. In such systems, the maximum quantum-mechanical value of the Leggett-Garg (LG) correlator  $K$  is  $K_L = 3/2$ . This was called the *Lüders bound* in Ref. [19] and follows as the temporal analogue [20] of the Tsirelson bound of the corresponding Bell inequality [21–23]. It is known that  $K_L$  bounds the LGI for quantum systems of arbitrary size provided that the measurements are genuinely dichotomic, i.e. can be modeled with exactly two projection operators [24]. Recently, however, it was predicted that values of  $K$  exceeding  $K_L$  are possible for multi-level systems when the measurement apparatus provides more information than a single bit, and is thus modeled with more than two projectors [19]. In particular, for a three-level system with measurements decom-

posed as three orthogonal projectors (each nevertheless associated with a value of either  $Q = +1$  or  $Q = -1$ ) it was predicted that the maximum value of the LG correlator is  $K^{\max} = 2.1547$  [19].

A small number of experiments have been performed on multi-level systems [25, 26], but these have only tested with LGI with two-projector measurements and were hence restricted to  $K \leq K_L$ . Recently, a three-level nuclear magnetic resonance (NMR) system was studied [27] for which a theoretical maximum violation of  $K = 1.7566 > K_L$  was predicted. However, no evidence of violations greater than the Lüders bound was found in the experiment. Violations exceeded  $K_L$  have recently been theoretically studied in multi-qubit systems [28].

In this paper, we report on an LG experiment with single photons that implements a three-level quantum system measured with three orthogonal projectors. Our main result is the observation of a value of the LG correlator  $K = 1.97 \pm 0.06$ , which clearly represents a significant enhancement over the Lüders value bound. We also consider a quantum-witness [29] (or no-signalling-in-time [30]) test for our system. This is based on the same assumptions as the LGIs but is simpler and is in some ways preferable [31]. In contrast with our results for the LGI, where the measured violation was still lower than the theoretical maximum for a three-level system measurement, our measured value for the quantum witness saturates the predicted theoretical maximum [32], and presents a significant enhancement over the hitherto-observed value for a two-projector measurement [26].

We obtain these value using *ideal negative measurements* (INMs) [3]. As in Refs. [12, 26, 27], these allow us to acquire information about the system (here, the photon) without interacting with it directly, and thus take measures to address the “clumsiness loophole” [33].

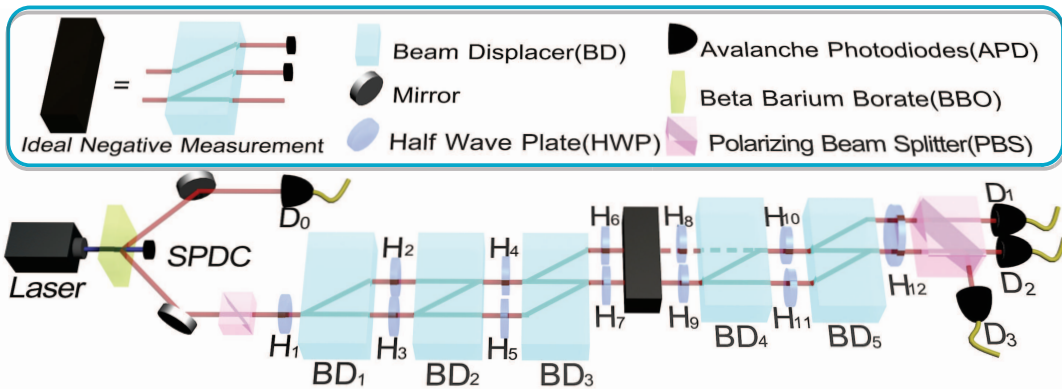


FIG. 1. Experimental setup for the LGI and quantum-witness tests. The heralded single photons are created via type-I SPDC in a BBO crystal and are injected into the optical network. The first PBS, HWP ( $H_1$ ) and  $BD_1$  are used to generate the initial qutrit state. The HWPs ( $H_2$ - $H_7$ ) and  $BD_2$ - $BD_3$  are used to realize the evolution operation  $U_1$ , while  $H_8$ - $H_{12}$  and  $BD_4$ - $BD_5$  are used to realize  $U_2$ . The projective measurement at  $t_3$  is realized via the second PBS which maps the basis states of the qutrit into three spatial modes. Detecting heralded single photons means in practice registering coincidences between the trigger detector  $D_0$  and each of the detectors for measurement  $D_1$ ,  $D_2$ , and  $D_3$ . The ideal negative measurement at time  $t_2$  is realized by blocking channels, two at a time. Here we show an example of blocking channels  $A$  and  $B$  such the probabilities  $P_{32}(n_3, n_2 = C)$  are obtained.

Our interferometric set-up makes the designation of our measurements as INM extremely clear-cut. These results underline the difference between Bell and LG inequalities and hence spatial and temporal correlations in quantum mechanics.

*Three-level LGI test:-* We begin with a common simplification [10, 26, 28] and assume the coincidence of state preparation with measurement at  $t_1$ . By defining  $Q(t_1) = 1$  the LGI reads

$$K \equiv \langle Q(t_2) \rangle + \langle Q(t_3)Q(t_2) \rangle - \langle Q(t_3) \rangle \leq 1. \quad (1)$$

We consider a system in which we measure a trichotomous variable  $n \in \{A, B, C\}$ . We connect with the LGI framework by introducing the mapping of a measurement of  $n_i$  at times  $t_i$  ( $i = 2, 3$ ) onto the value  $Q_i = Q(t_i) = q(n_i, t_i) \in \{-1, +1\}$ . This mapping leaves the classical upper bound unaffected.

To construct the LGI of Eq. (1) we require two distinct types of measurement set-up. In the first we measure the state of the system at time  $t_3$  and obtain  $P_3(n_3)$ , the probability to find state  $n_3 = A, B, C$  at time  $t_3$ . We then construct  $\langle Q(t_3) \rangle = \sum_{n_3} q(n_3, t_3)P_3(n_3)$ . In a second configuration we measure at times  $t_2$  and  $t_3$  to obtain  $P_{32}(n_3, n_2)$ , the joint probability to obtain  $n_2$  and  $n_3$  at these times. The correlation function can then be written as  $\langle Q(t_2) \rangle = \sum_{n_3, n_2} q(n_2, t_2)P_{32}(n_3, n_2)$  and  $\langle Q(t_3)Q(t_2) \rangle = \sum_{n_3, n_2} q(n_3, t_3)q(n_2, t_2)P_{32}(n_3, n_2)$ .

*Quantum violations:-* We now consider an idealised three-level quantum system, or qutrit, with states  $|n\rangle$ ;  $n = A, B, C$ . We prepare the system in state  $|C\rangle$  and let the unitary time-evolution operator between time

$t_1$  and  $t_2$  be

$$U_1 = \begin{pmatrix} \cos \theta & 0 & \sin \theta \\ \sin \theta \sin \phi & \cos \phi & -\cos \theta \sin \phi \\ -\sin \theta \cos \phi & \sin \phi & \cos \theta \cos \phi \end{pmatrix}, \quad (2)$$

in the basis  $|A\rangle = (1, 0, 0)^T$ ,  $|B\rangle = (0, 1, 0)^T$ ,  $|C\rangle = (0, 0, 1)^T$ . Following Ref. [32], we take the time evolution operator between  $t_2$  and  $t_3$  to be  $U_2 = U_1^\dagger$ .

Choosing the measurement outcomes for the LGI to be  $q(n_i = A, t_i) = q(n_i = B, t_i) = 1$  and  $q(n_i = C, t_i) = -1$  for  $i = 2, 3$ , we obtain the correlation functions  $\langle Q(t_3) \rangle = -1$ ,  $\langle Q(t_2) \rangle = \sin^2 \theta - \cos^2 \theta \cos 2\phi$ , and

$$\langle Q(t_3)Q(t_2) \rangle = \cos 2\theta [\sin^2 \theta + \cos^2 \theta (\cos^4 \phi - \sin^4 \phi)].$$

The maximum value of the corresponding LGI is  $K = 2$ , which occurs for the evolution parameters  $\theta = \pi/4, 3\pi/4$  and  $\phi = \pi/2$ .

*Experimental results:-* We now describe our realisation of the above scenario with single photons, Fig. 1. The basis states  $|A\rangle$ ,  $|B\rangle$ , and  $|C\rangle$  are encoded respectively by the horizontal polarization of the heralded single photons in the upper mode, the horizontal polarization of the photons in the lower mode, and the vertical polarization of the photons in the lower mode. Heralded single photons are generated via a type-I spontaneous parametric down-conversion (SPDC). The polarization-degenerate photon pairs at a wavelength of 801.6nm are produced in SPDC using a 0.5mm-thick  $\beta$ -barium-borate (BBO) nonlinear crystal pumped by a diode laser with 90mW of power. With the detection of a trigger photon the signal photon is heralded for evolution and measurement [34]. The pump is filtered out with the help of an interference filter which restricts the photon bandwidth to 3nm. Initial

qutrit states are prepared by first passing the heralded single photons through a polarizing beam splitter (PBS), and a half-wave plate (HWP,  $H_1$ ) before being split by a birefringent calcite beam displacer (BD) into two parallel spatial modes, upper and lower, with vertically-polarized photons directly transmitted through the BD in the lower mode, and with horizontal photons undergoing a 3mm lateral displacement into an upper mode. In the current set-up we set PBS and  $H_1$  to give vertically-polarized photons, which then remain in the lower mode through  $BD_1$ .

The unitary evolution applied on a qutrit state can be decomposed into three unitary operations as [35, 36]

$$U_1 = \begin{pmatrix} 1 & 0 & 0 \\ 0 & -\sin\phi & \cos\phi \\ 0 & \cos\phi & \sin\phi \end{pmatrix} \begin{pmatrix} \cos\theta & \sin\theta & 0 \\ -\sin\theta & \cos\theta & 0 \\ 0 & 0 & 1 \end{pmatrix} \begin{pmatrix} 1 & 0 & 0 \\ 0 & 0 & 1 \\ 0 & 1 & 0 \end{pmatrix}, \quad (3)$$

each of which applies a rotation on two of the basis states, leaving the other unchanged. Each of them can be realized by two HWPs and subsequent BD. One of the HWPs is used to apply a rotation on two modes of the qutrit state and the other is used to compensate the optical delay. The setting angles of  $H_3$ ,  $H_4$  and  $H_7$  can be calculated by the parameters  $\theta$  and  $\phi$  of the unitary operations. Whereas  $H_2$ ,  $H_5$  and  $H_6$  are used to compensate the optical delay. The  $BD_2$  and  $BD_3$  are used to split the photons with different polarizations into different spatial modes and to combine the photons with certain two of the polarization modes in the same spatial mode. Then two-mode (polarization mode) transformations can then be implemented using wave plates acting on the two polarization modes propagating in the same spatial mode. The evolution  $U_2$  is similarly realized by the HWPs ( $H_8$ - $H_{12}$ ) and BDs ( $BD_4$  and  $BD_5$ ).

For the first measurement setup, we perform projective measurements on the output states to obtain the probabilities  $P_3(n_3, t_3)$ . The second PBS is used to map the basis states of qutrit into three spatial modes and to accomplish the projective measurement. The photons are detected by single-photon avalanche photodiodes (APDs), in coincidence with the trigger photons. The probability of the photons being measured in  $|n\rangle$  ( $n = A, B, C$ ) is obtained by normalizing photon counts in the certain spatial mode to total photon counts. The count rates are corrected for differences in detector efficiencies and losses before the detectors. We assume that the lost photons would have behaved the same as the registered ones (fair sampling). Experimentally this trigger-signal photon pair is registered by a coincidence count at APD with 7ns time window. Total coincidence counts are about 14000 over a collection time of 7s.

For the second measurement setup, from which we derive  $P_{32}(n_3, n_2)$ , combines a projective measurement at  $t_3$ , as above, with an INM at  $t_2$  between the evolutions  $U_1$  and  $U_2$ . The INM are realised by placing Blocking

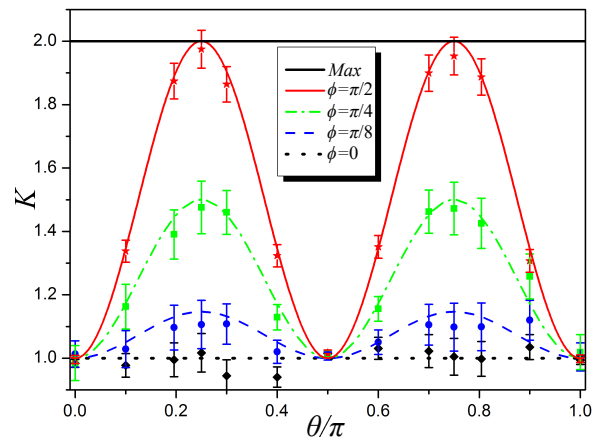


FIG. 2. Experimentally-determined values of the LG correlator  $K$  for the three-level system with time evolution described by the parameters  $\phi$  and  $\theta$ . Theoretical predictions are represented by solid lines and the experimental results by symbols. Error bars indicate the statistical uncertainty based on the assumptions of Poissonian statistics. The maximum measured value of the LG correlator occurs at  $\{\phi, \theta\} = \{\pi/2, \pi/4\}$  and has value  $K = 1.97 \pm 0.06$ , as compared with the theoretical maximum value of 2. This represents a significant enhancement over the Lüders bound of  $K_L = 3/2$ .

elements into the optical paths [37]. With, for example, the channels  $A$  and  $B$  blocked, we obtain the probabilities  $P_{32}(n_3, n_2 = C)$  without the measurement apparatus having interacting with the photon. In our experiment, this blocking is realized by a BD following by an iris. The BD is used to map the basis states of qutrit to three spatial modes and the iris is used to block photons in two of the three spatial modes and let the photons in the rest one pass through. By changing the position of the iris, we can block any two of the channels and let the photons in the rest one pass through for the next evolution.

Figure 2 shows the observed values of  $K$  as functions of  $\theta$  and  $\phi$ . Maximum violations are found for  $\phi = \pi/2$  with values  $K = 1.97 \pm 0.06$  at  $\theta = \pi/4$  and  $K = 1.95 \pm 0.06$  at  $\theta = 3\pi/4$ , in close agreement with the theoretical prediction. Error bars indicate the statistical uncertainty, based on the assumption of Poissonian statistics. The main deviation from theory arises in the first measurement setup where, by construction, the final state should be the same as the initial state such that  $\langle Q(t_3) \rangle = -1$ . However, due to imperfection in the cascaded interferometers in this setup,  $P_3(n_3 = C)$  is smaller than 1 and we obtain  $\langle Q(t_3) \rangle = 0.977 \pm 0.003$  at  $\{\phi, \theta\} = \{\pi/2, \pi/4\}$ . In the second measurement setup, there is no cascaded interferometer, and these effects are reduced.

*Quantum witness:-* Whilst the above set-up does not saturate the theoretical three-level maximum for the LGI,

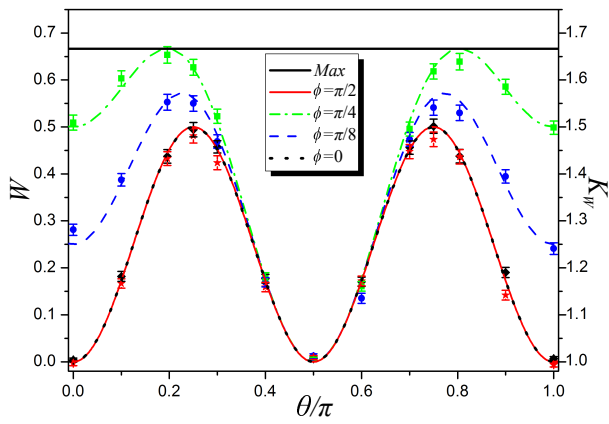


FIG. 3. The experimentally-determined values of the quantum witness  $W$  and the corresponding LGI  $K_W = 1 + W$  for our three-level system. The maximum value of the quantum witness is  $W = 0.65 \pm 0.02$ , which occurs for evolution parameters  $\{\phi, \theta\} = \{\pi/4, \arccos \sqrt{2/3}\}$ . This saturates the theoretical maximum of  $W = 2/3$  for a three-level system. The corresponding maximum value of the LGI is  $K_W = 1.65 \pm 0.02$ .

it does do so for the quantum witness

$$W \equiv P_3(n_3 = C) - \sum_{n_2} P_{32}(n_3 = C, n_2), \quad (4)$$

based on registering the state  $n_3 = C$ . Under macrorealism and non-invasive measurability, we have the equality  $W = 0$ . This witness can be constructed from the same probabilities as used in the LGI test and these results are shown in Fig. 3. Theory [32] predicts a maximum value of this witness should occur for the parameters  $\phi = \pi/4$  and  $\theta = \arccos \sqrt{2/3}$  and  $\theta = \pi - \arccos \sqrt{2/3}$ . At these points we observe the values  $W = 0.65 \pm 0.02$  and  $W = 0.64 \pm 0.02$ . This agrees well with the theoretical value of  $W = 2/3$ , which is the maximum possible value for a three-level system.

We can related this quantum witness directly to an LGI inequality if we choose measurement value assignments  $q(n_2, t_2) = 1$  at  $t_2$  (a blind measurement) [26], and  $q(n_3, t_3) = \delta_{n_3, C}$ . In this case, the LGI of Eq. (1) reduces to

$$K_W = 1 + W \leq 1. \quad (5)$$

Thus the value by which the witness exceeds zero is the extent to which the corresponding LGI is violated. The maximum violation of this LGI with this measurement assignment is thus  $K_W = 1.65 \pm 0.02$ .

*Discussion.-* We have demonstrated experimentally a violation of LGI in a three-level system and obtained a value of the LGI correlator greatly in excess of the Lüders bound  $K_L = 3/2$ , familiar from studies of two-level systems. We have also demonstrated violations of the quantum-witness equality, up to the theoretical maximum for a three-level system, and again, in excess of

what is possible for two-level systems. These enhancement arises because here the decisive  $t_2$ -measurement admits three distinct measurement outcomes, rather than the usual two. Under this measurement, the collapse of the wave function is complete, rather than partial (as it would be under two projectors), and this additional information gain enables the enhanced violation. Our results provide an experimental demonstration of the difference between spatial and temporal correlations in quantum mechanics, since the (spatial) Tsirelson bound in the corresponding Bell inequality is fixed at  $3/2$ , irrespective of the number of projectors. They also demonstrate that post-quantum effects are not needed to obtain these enhanced violations [38].

Classical invasive measurements can give violations of the LGI, all the way up the algebraic bound [39]. It is therefore important to ensure the non-invasivity of the measurements in any LGI test. Whilst no known scheme can completely rule out such invasivity [40], we have used INMs here which rule out the direct influence of the measurements on the particle themselves.

We would like to thank Neill Lambert for helpful discussions. We acknowledge support by NSFC (Nos. 11474049 and 11674056), NSFJS (No. BK20160024), and the Open Fund from State Key Laboratory of Precision Spectroscopy, East China Normal University.

\* gnep.eux@gmail.com

- [1] J. S. Bell, *Physics* **1**, 195 (1964).
- [2] M. Giustina, M. A. M. Versteegh, S. Wengerowsky, J. Handsteiner, A. Hochrainer, K. Phelan, F. Steinlechner, J. Kofler, J.-Å. Larsson, C. Abellán, W. Amaya, V. Pruneri, M. W. Mitchell, J. Beyer, T. Gerrits, A. E. Lita, L. K. Shalm, S. W. Nam, T. Scheidl, R. Ursin, B. Wittmann, and A. Zeilinger, *Phys. Rev. Lett.* **115**, 250401 (2015); L. K. Shalm, E. Meyer-Scott, B. G. Christensen, P. Bierhorst, M. A. Wayne, M. J. Stevens, T. Gerrits, S. Glancy, D. R. Hamel, M. S. Allman, K. J. Coakley, S. D. Dyer, C. Hodge, A. E. Lita, V. B. Verma, C. Lambrocco, E. Tortorici, A. L. Migdall, Y. Zhang, D. R. Kumor, W. H. Farr, F. Marsili, M. D. Shaw, J. A. Stern, C. Abellán, W. Amaya, V. Pruneri, T. Jennewein, M. W. Mitchell, P. G. Kwiat, J. C. Bienfang, R. P. Mirin, E. Knill, and S. W. Nam, *Phys. Rev. Lett.* **115**, 250402 (2015).
- [3] A. J. Leggett and A. Garg, *Phys. Rev. Lett.* **54**, 857 (1985); *Phys. Rev. Lett.* **59**, 1621 (1987).
- [4] C. Emary, N. Lambert, and F. Nori, *Rep. Prog. Phys.* **77**, 016001 (2015).
- [5] A. J. Leggett, *J. Phys.: Condens. Matter* **14**, R415 (2002).
- [6] A. Palacios-Laloy, F. Mallet, F. Nguyen, P. Bertet, D. Vion, D. Esteve, and A. N. Korotkov, *Nat. Phys.* **6**, 442 (2010).

- [7] G. Waldherr, P. Neumann, S. F. Huelga, F. Jelezko, and J. Wrachtrup, *Phys. Rev. Lett.* **107**, 090401 (2011).
- [8] V. Athalye, S. S. Roy, and T. S. Mahesh, *Phys. Rev. Lett.* **107**, 130402 (2011).
- [9] J.-S. Xu, C.-F. Li, X.-B. Zou, and G.-C. Guo, *Sci. Rep.* **1**, 101 (2011).
- [10] M. E. Goggin, M. P. Almeida, M. Barbieri, B. P. Lanyon, J. L. O’Brien, A. G. White, and G. J. Pryde, *Proc. Natl. Acad. Sci.* **108**, 1256 (2011).
- [11] J. Dressel, C. J. Broadbent, J. C. Howell, and A. N. Jordan, *Phys. Rev. Lett.* **106**, 040402 (2011).
- [12] G. C. Knee, S. Simmons, E. M. Gauger, J. J. L. Morton, H. Riemann, N. V. Abrosimov, P. Becker, H.-J. Pohl, K. M. Itoh, M. L. W. Thewalt, G. A. D. Briggs, and S. C. Benjamin, *Nat. Commun.* **3**, 606 (2012).
- [13] J. P. Groen, D. Ristè, L. Tornberg, J. Cramer, P. C. de Groot, T. Picot, G. Johansson, and L. DiCarlo, *Phys. Rev. Lett.* **111**, 090506 (2013).
- [14] H. Katiyar, A. Shukla, K. R. K. Rao, and T. S. Mahesh, *Phys. Rev. A* **87**, 052102 (2013).
- [15] A. Asadian, C. Brukner, and P. Rabl, *Phys. Rev. Lett.* **112**, 190402 (2014).
- [16] Z.-Q. Zhou, S. F. Huelga, C.-F. Li, and G.-C. Guo, *Phys. Rev. Lett.* **115**, 113002 (2015).
- [17] G. C. Knee, K. Kakuyanagi, M.-C. Yeh, Y. Matsuzaki, H. Toida, H. Yamaguchi, S. Saito, A. J. Leggett, and W. J. Munro, *Nat. Commun.* **7**, 13253 (2016).
- [18] J. Formaggio, D. Kaiser, M. Murskyj, and T. Weiss, *Phys. Rev. Lett.* **117**, 050402 (2016).
- [19] C. Budroni and C. Emary, *Phys. Rev. Lett.* **113**, 050401 (2014).
- [20] T. Fritz, *New J. Phys.* **12**, 083055 (2010).
- [21] B. Cirel’son, *Lett. Math. Phys.* **4**, 93 (1980).
- [22] H. S. Poh, S. K. Joshi, A. Cerè, A. Cabello, and C. Kurtsiefer, *Phys. Rev. Lett.* **115**, 180408 (2015).
- [23] M. Navascués, S. Pironio, and A. Acín, *New J. Phys.* **10**, 073013 (2016).
- [24] C. Budroni, T. Moroder, M. Kleinmann, and O. Gühne, *Phys. Rev. Lett.* **111**, 020403 (2013).
- [25] R. E. George, L. M. Robledo, O. J. E. Maroney, M. S. Blok, H. Bernien, M. L. Markham, D. J. Twitchen, J. J. L. Morton, G. A. D. Briggs, and R. Hanson, *Proc. Natl. Acad. Sci.* **110**, 3777 (2013).
- [26] C. Robens, W. Alt, D. Meschede, C. Emary, and A. Alberti, *Phys. Rev. X* **5**, 011003 (2015).
- [27] H. Katiyar, A. Brodutch, D. Lu, and R. Laflamme, arXiv:1606.07151v1 [quant-ph].
- [28] N. Lambert, K. Debnath, A. F. Kockum, G. C. Knee, W. J. Munro, and F. Nori, *Phys. Rev. A* **94**, 012105 (2016).
- [29] C.-M. Li, N. Lambert, Y.-N. Chen, G.-Y. Chen, and F. Nori, *Sci. Rep.* **2** (2012).
- [30] J. Kofler and Č. Brukner, *Phys. Rev. A* **87**, 052115 (2013).
- [31] L. Clemente and J. Kofler, *Phys. Rev. Lett.* **116**, 150401 (2016).
- [32] G. Schild and C. Emary, *Phys. Rev. A* **92**, 032101 (2015).
- [33] M. M. Wilde and A. Mizel, *Found. Phys.* **42**, 256 (2011).
- [34] P. Xue, R. Zhang, H. Qin, X. Zhan, Z. H. Bian, J. Li, and B. C. Sanders, *Phys. Rev. Lett.* **114**, 140502 (2015).
- [35] M. Reck, A. Zeilinger, H. J. Bernstein, and P. Bertani, *Phys. Rev. Lett.* **73**, 58 (1994).
- [36] K. Wang, X. Zhan, Z. Bian, J. Li, Y. Zhang, and P. Xue, *Phys. Rev. A* **93**, 052108 (2016).
- [37] C. Emary, N. Lambert, and F. Nori, *Phys. Rev. B* **86**, 235447 (2012).
- [38] B. Dakić, T. Paterek, and Č. Brukner, arXiv:1308.2822 (2013).
- [39] A. Montina, *Phys. Rev. Lett.* **108**, 160501 (2012).
- [40] Results such as Ref. [33] and Ref. [17] reduce the “size” the clumsiness loophole, but do not close it altogether.